Dynamics of vortex nucleation in nanomagnets with broken symmetry

Jaroslav Tóbik,[1,*] Vladimír Cambel,[1] and Goran Karapetrov[1,2]

[1]*Institute of Electrical Engineering, Slovak Academy of Sciences, Dúbravská cesta 9, SK-841 04 Bratislava, Slovakia*

[2]*Department of Physics, Drexel University, 3141 Chestnut Street, Philadelphia, Pennsylvania 19104, USA*

(Received 19 March 2012; revised manuscript received 14 October 2012; published 31 October 2012)

We investigate the dynamics of magnetic vortex nucleation in sub-100-nm mesoscopic magnets with the aim of establishing an independent control of vortex polarity and chirality. We consider the dynamic behavior of the vortex spin structure in an object with broken symmetry—a Pacman-like nanomagnet shape—proposing a model based on classical electrodynamics and providing a proof by conducting micromagnetic calculations. The model provides evidence that the desired vortex chirality and polarity could be established by applying solely quasistatic in-plane magnetic field along specific directions with respect to the structure's asymmetry. We identify the modes of vortex nucleation that are robust against external magnetic field noise. These vortex nucleation modes are common among a wide range of sub-100-nm magnets with broken rotational symmetry. The results could lead to the practical realization of high density magnetic memories based on magnetic vortices.

DOI: 10.1103/PhysRevB.86.134433 PACS number(s): 75.75.Fk, 75.60.Jk, 75.78.Cd

Confinement leads to fundamental changes in the physical behavior of materials due to the increased role of the surface. In mesoscopic magnetic materials such changes in the energy landscape could lead to novel magnetic spin configurations such as vortices. The equilibrium properties of these topological states are governed by both the properties of the magnetic material and the geometry of the object. On the other hand, confinement also leads to the distinct dynamic behavior of these topological states since the available energy levels are very much limited. The transition probabilities between different states can thus be controlled by careful engineering of the geometry of the mesoscopic object. Here we show that by tailoring the geometry of the mesoscopic magnet one can produce deterministic dynamic switching between well-defined degenerate topological states using only in-plane magnetic fields. We present an analytical model that explains the mechanism of the vortex nucleation and origin of robustness of the vortex polarization. Confirmation of the model is accomplished by conducting micromagnetic simulations. The findings could lead to practical realization of a two-bit magnetic memory cell based on a controlled setting and the readout of the polarity and chirality of the magnetic vortex.

Controlled manipulation of magnetic domains in ferromagnet nanostructures have recently opened opportunities for novel fast, high-density, and low-power memories with novel architectures.[1–3] Any perspective magnetic memory architecture, such as submicron nonvolatile magnetic memory, has to have (1) a well-defined switching field used to set the memory bits, and (2) a reproducible switching behavior using a simple sequence of external magnetic field pulses. Therefore, the dynamics of the switching between different ground states has to be understood in detail.

Recent advances in fabrication technology at nanoscale have enabled studies of magnetic systems that are well defined in all three dimensions on a nanometer length scale ($<$100 nm).[4,5] The size reduction of nanomagnets leads to novel spin topological states such as the vortex state, *C* state, *S* state, flower state, and so on,[6] and to simplified transitions between these states in the external magnetic field. The transition between ground states in such nanomagnets is of fundamental importance.[7,8] It is governed by competition between the magnetostatic energy and exchange energy, and it is influenced by the magnetic material used and by the choice of the nanomagnet shape. For example, the magnetization of disks in a zero field can be oriented in-plane, out-of-plane, or a vortex state can be created depending on the disk diameter and thickness.[4,9] In the disk the flux-closure magnetic state reduces the long-range stray fields (i.e., reduces the magnetostatic interaction between neighboring disks). Therefore, such disk magnetic systems have a potential for high-density magnetic storage elements, with bits represented by the chirality and polarity of a basic vortex state.

In submicron-sized disks four possible states have to be controlled. It was shown experimentally that in the nanomagnets with broken rotational symmetry, chirality can be controlled easily by the in-plane field of a selected direction.[10–13] At the same time the polarity of the vortex core, which represents the second bit, can be controlled by an out-of-plane magnetic field,[13] spin-polarized current,[8] high-frequency in-plane magnetic field,[14] or by an in-plane magnetic pulse of precisely defined amplitude and duration.[15]

In our previous work we have proposed a prospective shape of a nanomagnet with broken symmetry which permits the control of chirality and polarity bits by the application of the in-plane field only.[16] In this paper we analyze the mechanisms that establish specific chirality and polarity values in such a Pacman-like (PL) nanomagnet by taking a closer look at the energies and dynamics that govern the switching processes. Using an *analytical model* we show that the polarity and the chirality of the vortex core nucleated in the decreasing in-plane magnetic field is implicitly defined by the direction of the magnetic field with respect to the missing sector of the PL nanomagnet.

We consider a magnetic dot of cylindrical shape. To construct a PL structure it is necessary to remove an outer sector that is 45° wide, and has 1/3 of the disk radius (see Fig. 1). Due to a symmetry analysis that will be presented later, we choose the orientation of the x,z axes such that they define the mirror symmetry plane σ_y, which leaves the PL object

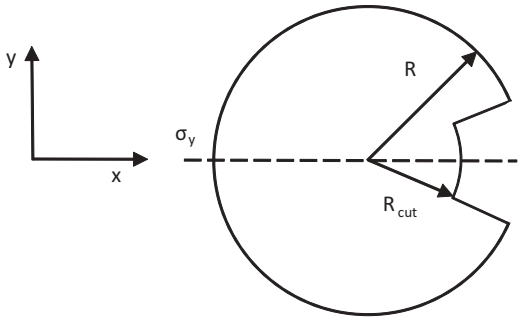

FIG. 1. Geometry of Pacman-like nanomagnet. The structure is symmetric with respect to reflection plane σ_y.

invariant. Another symmetry operation is mirroring through the plane x,y noted in the following text by σ_z.

First, we define polarity $\vec{\pi}[\vec{f}]$ and chirality $\vec{\chi}[\vec{f}]$ vectors as functionals of an arbitrary vector field $\vec{f}$:

$$\vec{\pi}[\vec{f}] = \frac{1}{\Omega}\int \vec{f}(\vec{r})d\Omega,$$
$$\vec{\chi}[\vec{f}] = \int \vec{r}\times(\vec{f}(\vec{r})-\vec{\pi})d\Omega. \quad (1)$$

Polarity is just th simple average value of the field, while chirality resembles the definition of the momentum of quantity $\vec{f}$ in classical mechanics. The subtraction of polarity in the expression for chirality is necessary due to chirality invariance with respect to the origin coordinate system choice. Mostly we are interested in the z component of polarity and chirality. The integration domain Ω is over the volume of the PL nanomagnet.

Let us consider that the nanomagnet is placed in a strong in-plane magnetic field that has an angle φ with the x axis. To emulate the magnetic response by the missing sector, we can consider the PL nanomagnet as a superposition of a full disk and a set of microscopic magnetic moments in a removed sector. These additional moments have to have the same value and to be oriented in the opposite direction to the magnetic

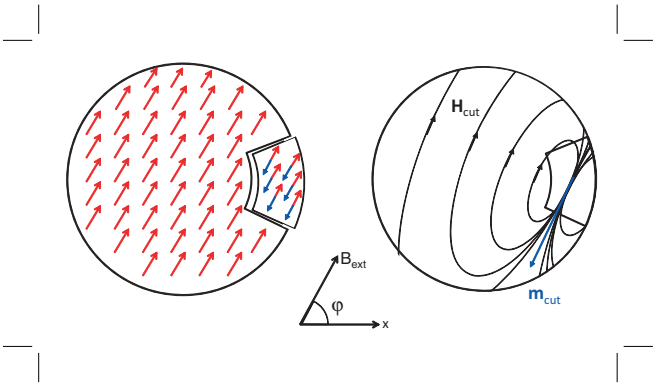

FIG. 2. (Color online) (a) The magnetization of the Pacman-like nanomagnet is a superposition of the uniform magnetization of a full disk (red arrows) and the magnetization of the missing sector that is equal and opposite to the one of the full disk. (b) The sum of the compensation moments in the sector creates a dipole $m_{\rm cut}$ which asymmetrically interacts with the local magnetization in the nanomagnet.

moments in the disk (Fig. 2). In the first approximation all microscopic moments are parallel. Neglecting higher than dipolar moments, the missing sector behaves as a dipole with a moment $\vec{m}_{\rm cut}$ positioned in the center of mass of the sector $\vec{r}_{\rm T}$:

$$\vec{m}_{\rm cut} = -\int \vec{M}d\Omega' \quad \vec{r}_{\rm T} = \frac{1}{\Omega'}\int \vec{r}d\Omega'. \quad (2)$$

The minus sign reflects that dipoles of opposite orientation have to be added to eliminate the dipoles in the missing sector (see Fig. 2). The integration is over the volume of the missing sector Ω'.

To calculate the magnetic field of the PL nanomagnet, consider first the full disk. In magnetic fields exceeding the saturation field the magnetic polarization $\vec{M}$ is parallel to the direction of the applied field $\vec{H}_{\rm ext}$ throughout the disk volume. The internal magnetic field $\vec{H}$ is also uniformly oriented in parallel with $\vec{M}$. As a small piece of material is removed, all the fields change slightly. To correct the internal magnetic field, the field of magnetic moment $\vec{m}_{\rm cut}$ given by Eq. (2) has to be added to the originally homogeneous internal field of the full disk. The removed part thus creates a dipole which induces magnetic field with nonzero chirality $\chi[\vec{H}]$, if $\varphi \neq 0°, 180°$. Since dipoles partially follow the field orientation, the nonzero chirality of $\vec{M}$ is expected.

Next, we explain qualitatively the mechanism which determines vortex core polarity. Taking into consideration magnetostatics only, the state with positive polarity $\pi[\vec{M}]$ is energetically equivalent to the state with negative polarity $-\pi[\vec{M}]$, if no external field in the z direction is applied. That can be easily seen by writing the total energy functional

$$E = \frac{\mu_0}{4\pi}\int\int\left(\frac{\vec{M}\cdot\vec{M}'}{|\vec{r}-\vec{r}'|^3} - \frac{3\vec{M}\cdot(\vec{r}-\vec{r}')\vec{M}'\cdot(\vec{r}-\vec{r}')}{|\vec{r}-\vec{r}'|^5}\right)d\Omega d\Omega'$$
$$+ A\int(\nabla\vec{M})^2 d\Omega - \int \vec{H}_{\rm ext}\cdot\vec{M}d\Omega. \quad (3)$$

Changing the sign of M_z does not change the first two integrals of Eq. (3) since these two parts of the energy functional are quadratic in M_z and its derivative, respectively. The only linear part in M_z is in the third integral. But a change of sign of M_z would not influence the total energy because $H_{\rm ext}$ has no z component. The integration domain Ω is not changed by reversing z because the symmetry operation σ_z—the reflection from the plane xy transforms the PL nanomagnet to itself.

The final state of the vortex core polarization is determined by magnetization dynamics. The time evolution of magnetization is described by the phenomenological Landau-Lifshitz-Gilbert (LLG) equation

$$\frac{\partial\vec{M}}{\partial t} = -\gamma\vec{M}\times\vec{H}_{\rm eff} + \alpha\left(\vec{M}\times\frac{\partial\vec{M}}{\partial t}\right). \quad (4)$$

Here we show that this equation itself contains a polarity symmetry-breaking mechanism. First, we apply a strong external in-plane field in the direction that has an angle φ with the x axis (Fig. 2). Then we slowly (adiabatically) decrease the external field amplitude to the level that is just above the vortex nucleation field. By adiabatic field change we mean that the change of the external field with time is so slow that the energy dissipation keeps the system very close to the local minimum at

all times. Then $\frac{\partial \vec{M}}{\partial t} \approx 0$ everywhere. Any dynamics means also the dissipation of energy due to the term that is proportional to α in Eq. (4). Therefore, at local minima also $\vec{H}_{\text{eff}}$ is parallel to magnetization $\vec{M}$, otherwise it is not possible to satisfy Eq. (4) with vanishing left side. We note this effective field $\vec{H}_{\text{eff}}^{\parallel}$. Now, having $\vec{H}_{\text{ext}}$ just above the nucleation field, we decrease the external field by a small value $\Delta\vec{H}$. To the first approximation the effective field is $\vec{H}_{\text{eff}} = \vec{H}_{\text{eff}}^{\parallel} + \Delta\vec{H}$. When looking at the dynamics of local magnetic moments shortly after the external field is decreased, we can neglect the damping term in the LLG equation since $\alpha \ll 1$. The torque on the z component of magnetization is then given by the equation

$$\frac{\partial M_z}{\partial t} = -\gamma(M_x \Delta H_y - M_y \Delta H_x). \tag{5}$$

The right-hand side of Eq. (5) is not zero locally, nor it is on average, due to the asymmetry of the PL nanomagnet with respect to the direction of the applied field (if $\varphi \neq 0°, 180°$). If the actual value of the external field is lower than the nucleation field, the nonzero polarity of the nanomagnet starts to evolve. From pure energy considerations, the two vortex states with opposite polarity are energetically equivalent. Looking at the time-evolution equation (4), especially at its first-order approximation (5), one sees that the magnetization is driven towards the well-defined direction by the geometric asymmetry of the PL nanomagnet. The direction of the initial polarity evolution is obtained by the volume integration of Eq. (5).

The confirmation of the above model approximation can be obtained by numerical simulations. We have performed numerical simulations of the PL nanomagnet using the OOMMF software package.[17] The parameters used in the simulation are as follows: outer radius $R = 35$ nm, thickness (in the z direction, not shown) $h = 40$ nm. The material used in the calculations is Permalloy $Ni_{80}Fe_{20}$ (Py), with the following material parameters: exchange constant $A = 13 \times 10^{-12}$ J/m, saturated magnetization $M_s = 8.6 \times 10^5$ A/m, and Gilbert damping parameter $\alpha = 0.5$. Numerical simulations were done on a rectangular mesh of size 1 nm. To check the possible influence of the discretization, calculations with a PL nanomagnet rotated against the discretization mesh by 10° and 22.5° were performed. The same results for B_{in} within an error of 2 mT were achieved.

In Fig. 3 we show the dependence of the nucleation-field amplitude on the applied field direction. The nucleation field is defined as the applied magnetic field at which the nonzero z component of the magnetization polarity $\pi(\vec{M})$ appears. The external field is adiabatically decreasing from 150 mT to zero in the selected direction. By adiabatic change we mean the repeated process of decreasing the field by a 2 mT step, followed by full system relaxation.

We would like to note the symmetry properties of the PL nanomagnet. In Fig. 3 (top) each quadrant corresponds to a vortex ground state of the nanomagnet with the specific chirality and polarity shown in corresponding corners. The nanomagnet relaxes into that remanent state from a uniform magnetization along an angle within the specific quadrant. As can be seen in Fig. 3, the angular dependence of the nucleation field can be reconstructed from the dependence for $\varphi \in [0; \frac{\pi}{2}]$ by inversion and reflection through the xz plane

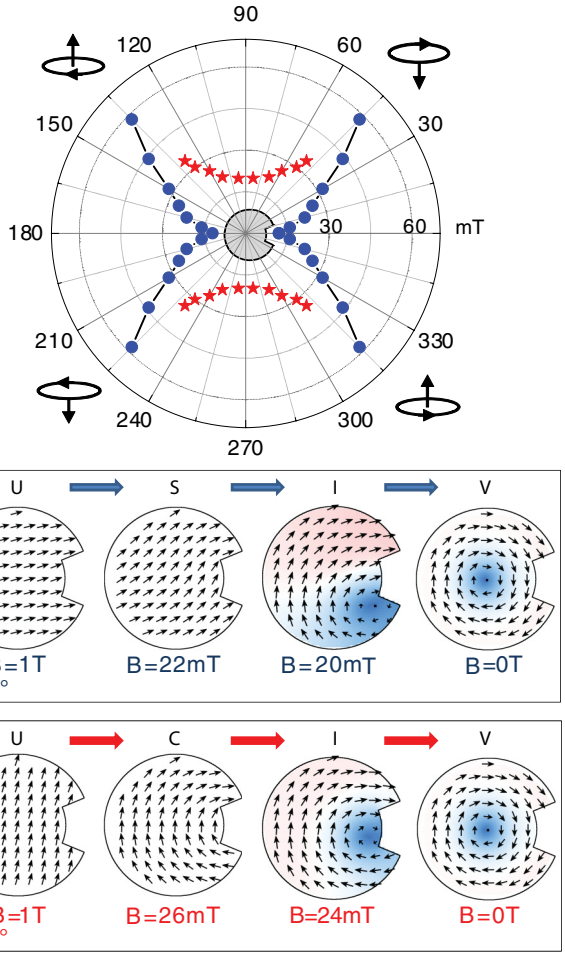

FIG. 3. (Color online) Top: Angular dependence of vortex nucleation field. Direction of the nucleated vortex polarity and chirality are also indicated for each quadrant. Bottom: Two different processes of vortex nucleation depending on the initial magnetization direction with respect to PL's symmetry plane ($\varphi = 15°$ and $\varphi = 75°$). From the uniform magnetization state (U) the magnetization transitions to S-shape (dots) or C-shape (stars) configurations and equilibrates to a vortex state (V) with specific polarity and chirality. The snapshot of the intermediate state (I) shows the position of vortex core nucleation.

σ_y. The inversion symmetry of the graph shown in Fig. 3 is the consequence of the time-reversal symmetry. The reflection symmetry with respect to the xz plane shown in Fig. 3 is related to the reflection from σ_y—the geometrical operation that transforms the PL nanomagnet to itself.

The simulation results show the existence of *two distinct vortex core nucleation regimes* [Fig. 3 (bottom)]. For large angles ($\varphi \in [50°; 90°]$) the vortex nucleates from the C-state magnetization pattern. This form of nucleation is not robust in the sense that even the small out-of-plane field $B_z \simeq 1$ mT is sufficient to alter the resulting polarity of the nucleated vortex along the direction of the applied field B_z (Fig. 4). Instead, for small angles ($\varphi \in [0°; 48°]$) the vortex nucleation path is different. Just above the vortex nucleation field, the magnetization of the PL nanomagnet forms an S state. This configuration consists of two regions with opposite signs of the curvature of field lines.[18] Meanwhile, there is only one curvature of field lines just below the vortex nucleation field.

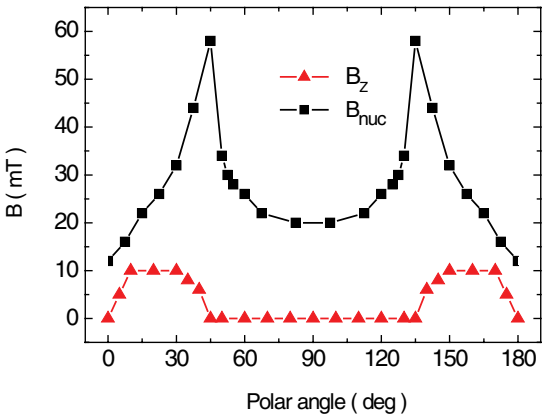

FIG. 4. (Color online) Angular dependence of the in-plane vortex nucleation field B_{nuc} and threshold out-of-plane field B_z necessary to reverse the polarity of the entering vortex.

The process of vortex core nucleation in this case involves the *reversal of magnetic moments* in a part of the nanomagnet. This reversal process proceeds through an out-of-plane motion of the local magnetic moments, resulting in robust vortex core polarization despite the presence of small external fields in the z direction. In Fig. 4 we show the angular dependence of the maximum external field B_z for which the PL nanomagnet is able to sustain nucleation of vortex polarity opposite to the direction of the applied external field.

The C and S shapes of magnetization can be explained by the position of perturbing dipole $\vec{m}_{\text{cut}}$. As can be seen from Fig. 2, the PL nanomagnet is divided into two domains with the opposite sign of the magnetic field circulation generated by $\vec{m}_{\text{cut}}$. The sizes of these two domains are determined by the orientation of $\vec{m}_{\text{cut}}$. However, the exchange interaction tends to align local moments in parallel, thus there exists a critical angle (around 48° in our geometry), beyond which the region with minor curvature does not exist. A detailed energy balance between the exchange and cavity (sector) demagnetization determines the scenario of vortex nucleation and its eventual robustness with respect to external perturbation.

We would like to point out that the adiabatic case discussed above describes the magnetization dynamics on the order of several nanoseconds. We also performed OOMMF simulations for the nonadiabatic case, when the change of the external magnetic field is faster than the local magnetization dynamics. We find that the final vortex state has the same angular dependence on the initial applied in-plane magnetic field as in the adiabatic case (Fig. 4). Moreover, the robustness of the transition is increased, as measured by the magnitude of the threshold out-of-plane B_z necessary to alter the final polarity. An intuitive understanding for the increased robustness can be inferred from Eq. (5): The initial impulse given to the system is proportional to the amplitude of the in-plane magnetic field step during which vortex nucleation occurs. This basically means that the PL nanomagnet is more stable when operated at higher switching speeds.

The analysis provided above has been performed without taking into account finite temperature effects. Preliminary estimates indicate that the results could be altered by thermal effects when the thermal energy is comparable to the energy cushion estimated by the opposite B_z necessary to alter the final polarity of the vortex state (Fig. 4). According to simulations, at room temperature the final polarity and chirality for applied fields at angles $-45^\circ \leqslant \varphi \leqslant 45^\circ$ do not change. A more complicated situation arises for other angles of the in-plane applied field, but the full analysis is beyond the scope of this work and will be addressed in the near future.

To summarize, in this work we provide simple arguments that elucidate the origin of driving mechanisms for the nucleation of magnetic vortex with controlled chirality and polarity. We also find the regime of the PL nanomagnet operation in which the final vortex state is independent on a weak disturbing external field. This is a promising finding to consider if using the PL nanomagnet as a memory element in bit-patterned media or as a generator of magnetic vortices of desired polarity and chirality for microwave applications. Weak interaction among the elements as well as robustness to small external field perturbations makes the PL nanomagnet very suitable for operation.

Finally, we note, that the sub-100-nm PL nanomagnet is not the only unique design offering control of chirality and polarity by in-plane magnetic field. Qualitatively similar results are obtained in simulations for different sizes and shapes of the missing sector. According to our model, the necessary ingredients are the symmetry of the object, the demagnetization field strength of the removed part, and shape anisotropy induced by the removed part. The robustness of vortex polarity against B_z is based on the vortex–antivortex annihilation during vortex core nucleation.

This work has been supported by the project CENTE II, Research & Development Operational Program funded by the ERDF, ITMS 26240120019, and by VEGA 2/0037/12.

*jaroslav.tobik@savba.sk

[1]S. S. Parkin, H. Hayashi, and L. Thomas, Science **320**, 190 (2008).

[2]K. S. Buchanan, P. E. Roy, M. Grimsditch, F. Y. Fradin, K. Yu. Guslienko, S. D. Bader, and V. Novosad, Nat. Phys. **1**, 172 (2005).

[3]C. A. Ross, H. I. Smith, T. Savas, M. Schattenburg, M. Farhoud, M. Hwang, M. Walsh, M. C. Abraham, and R. J. Ram, J. Vac. Sci. Technol. B **17**, 3168 (1999).

[4]S. H. Chung, R. D. McMichael, D. T. Pierce, and J. Unguris, Phys. Rev. B **81**, 024410 (2010).

[5]J. W. Lau and J. M. Shaw, J. Phys. D **44**, 303001 (2011).

[6]R. P. Cowburn, J. Phys. D **33**, 1R (2000).

[7]W. F. Brown, J. Appl. Phys. **39**, 993 (1968); K. Yu. Guslienko, K. S. Lee, and S. K. Kim, Phys. Rev. Lett. **100**, 027203 (2008); M. Bolte, G. Meier, B. Krüger, A. Drews, R. Eiselt, L. Bocklage, S. Bohlens,

T. Tyliszczak, A. Vansteenkiste, B. Van Waeyenberge, K. W. Chou, A. Puzic, and H. Stoll, *ibid.* **100**, 176601 (2008).

[8]K. Yamada, S. Kasai, Y. Nakatani, K. Kobayashi, H. Kohno, A. Thiaville, and T. Ono, Nat. Mater. **6**, 269 (2007).

[9]J. d'Albuquerque e Castro, D. Altbir, J. C. Retamal, and P. Vargas, Phys. Rev. Lett. **88**, 237202 (2002).

[10]M. Schneider, H. Hoffmann, and J. Zweck, Appl. Phys. Lett. **79**, 3113 (2001).

[11]T. Taniuchi, M. Oshima, H. Akinaga, and K. Ono, J. Appl. Phys. **97**, 10J904 (2005).

[12]P. Vavassori, R. Bovolenta, V. Metlushko, and B. Ilić, J. Appl. Phys. **99**, 053902 (2006).

[13]M. Jaafar, R. Yanes, D. Perez de Lara, O. Chubykalo-Fesenko, A. Asenjo, E. M. Gonzalez, J. V. Anguita, M. Vazquez, and J. L. Vicent, Phys. Rev. B **81**, 054439 (2010).

[14]K. S. Lee, K. Y. Guslienko, J. Y. Lee, and S. K. Kim, Phys. Rev. B **76**, 174410 (2007).

[15]R. Antos and Y. Otani, Phys. Rev. B **80**, 140404 (2009).

[16]V. Cambel and G. Karapetrov, Phys. Rev. B **84**, 014424 (2011).

[17]M. J. Donahue and D. G. Porter, *OOMMF User's Guide, Version 1.0*, Technical Report No. NISTIR 6376, National Institute of Standards and Technology, Gaithersburg, MD (1999).

[18]To be precise, we mean the curvature of field lines projected onto the xy plane since the concept of curvature with sign is meaningful for curves in two dimensions.